

Transfontanellar Contrast-enhanced US for Intraoperative Imaging of Cerebral Perfusion during Neonatal Arterial Switch Operation

Ferdinand Knieling, MD • Robert Cesnjevar, MD¹ • Adrian P. Regensburger, MD • Alexandra L. Wagner, MD • Ariawan Purbojo, MD • Sven Dittrich, MD • Frank Münch, MS • Antje Neubert, PhD • Joachim Woelfle, MD • Jörg Jüngert, MD* • André Rüffer, MD²*

From the Departments of Pediatrics and Adolescent Medicine (F.K., A.P.R., A.L.W., A.N., J.W., J.J.), Congenital Heart Surgery (R.C., A.P., F.M.), and Pediatric Cardiology (S.D.), University Hospital Erlangen, Friedrich-Alexander-Universität Erlangen-Nürnberg, Loschgstrasse 15, 91054 Erlangen, Germany; and Section for Congenital and Pediatric Cardiac Surgery, University Heart Center Hamburg, University Hospital Hamburg, Eppendorf, Hamburg, Germany (A.R.). Received August 18, 2021; revision requested October 22; revision received January 11, 2022; accepted February 2. **Address correspondence to** F.K. (e-mail: Ferdinand.Knieling@uk-erlangen.de).

¹**Current address:** Department of Paediatric Cardiothoracic Surgery, University Hospital Zürich, Zürich, Switzerland.

²**Current address:** Department of Pediatric Cardiac Surgery, University Hospital Aachen (UKA), RWTH Aachen University, Aachen, Germany.

F.K. and J.J. supported by the German Society for Ultrasound in Medicine (Deutsche Gesellschaft für Ultraschall in der Medizin). F.K. and A.P.R. supported by the Interdisciplinary Center for Clinical Research. F.K. supported by the ELAN fund Erlangen.

*J.J. and A.R. are co-senior authors.

Conflicts of interest are listed at the end of this article.

Radiology 2022; 000:1–9 • <https://doi.org/10.1148/radiol.212044> • Content codes: **PD** **NR** **US**

Background: Brain injury and subsequent neurodevelopmental disorders are major determinants for later-life outcomes in neonates with transposition of the great arteries (TGA).

Purpose: To quantitatively assess cerebral perfusion in neonates with TGA undergoing arterial switch operation (ASO) using transfontanellar contrast-enhanced US (T-CEUS).

Materials and Methods: In a prospective single-center cross-sectional diagnostic study, neonates with TGA scheduled for ASO were recruited from February 2018 to February 2020. Measurements were performed at five time points before, during, and after surgery (T_1 – T_5), and 11 perfusion parameters were derived per cerebral hemisphere. Neonate clinical characteristics, heart rate, mean arterial pressure, central venous pressure, near-infrared spectroscopy, blood gas analyses, ventilation time, time spent in the pediatric intensive care unit, and time in hospital were correlated with imaging parameters. Analysis of variance or a mixed-effects model were used for groupwise comparisons.

Results: A total of 12 neonates (mean gestational age, 39 6/7 weeks \pm 1/7 [SD]) were included and underwent ASO a mean of 6.9 days \pm 3.4 after birth. When compared with baseline values, T-CEUS revealed a longer mean time-to-peak (right hemisphere, 4.3 seconds \pm 2.1 vs 17 seconds \pm 6.4 [$P < .001$]; left hemisphere, 4.0 seconds \pm 2.3 vs 21 seconds \pm 8.7 [$P < .001$]) and rise time (right hemisphere, 3.5 seconds \pm 1.7 vs 11 seconds \pm 5.1 [$P = .002$]; left hemisphere, 3.4 seconds \pm 2.0 vs 22 seconds \pm 7.8 [$P = .004$]) in both cerebral hemispheres during low-flow cardiopulmonary bypass and hypothermia (T_b) for all neonates. Neonate age at surgery negatively correlated with T-CEUS parameters during ASO, as calculated with the area under the flow curve (AUC) during wash-in ($R = -0.60$, $P = .020$), washout ($R = -0.82$, $P = .002$), and both wash-in and washout ($R = -0.79$, $P = .004$). Mean AUC values were lower in neonates older than 7 days compared with younger neonates during wash-in ($[87 \text{ arbitrary units } \{au\} \pm 77] \times 10^3$ vs $[270 \text{ au} \pm 164] \times 10^3$, $P = .049$), washout ($[15 \text{ au} \pm 11] \times 10^3$ vs $[65 \text{ au} \pm 38] \times 10^3$, $P = .020$) and both wash-in and washout ($[24 \text{ au} \pm 18] \times 10^3$ vs $[92 \text{ au} \pm 53] \times 10^3$, $P = .023$).

Conclusion: Low-flow hypothermic conditions resulted in reduced cerebral perfusion, as measured with transfontanellar contrast-enhanced US, which inversely correlated with age at surgery.

Clinical trial registration no. NCT03215628

© RSNA, 2022

Online supplemental material is available for this article.

The prognosis of patients with congenital heart disease has substantially improved over the past several decades, especially due to advances in surgical techniques (1,2). Arterial switch operation (ASO) for transposition of the great arteries (TGA) attempts to re-establish the connection of pulmonary and systemic body circulation (3). Neurodevelopmental impairment, either from preexisting syndromic or genetic conditions or from complex surgical interventions, has become an important determinant for long-term

morbidity and mortality (4). For ASO, the age at repair was found to be predictive of future cognitive function (5). Refinements to the surgical procedures, such as the use of a low-flow cardiopulmonary bypass (CPB) in comparison with circulatory arrest, have improved early (6) and late neurologic outcomes (7).

Several imaging studies have tried to unravel the association between surgical interventions in congenital heart disease and possible later neurodevelopmental impairment

Abbreviations

ASO = arterial switch operation, AUC = area under the flow curve, CPB = cardiopulmonary bypass, PCO_2 = partial pressure of carbon dioxide, T-CEUS = transfontanellar contrast-enhanced US, TGA = transposition of the great arteries

Summary

Transfontanellar contrast-enhanced US enables intraoperative imaging and quantification of cerebral perfusion during neonatal heart surgery.

Key Results

- In a prospective study of 12 neonates undergoing heart surgery, transfontanellar contrast-enhanced US (T-CEUS) enabled quantification of cerebral perfusion undergoing arterial switch operation (ASO).
- Neonate age at surgery negatively correlated with T-CEUS flow parameters during ASO as calculated with area under the flow curve during both wash-in and washout ($R = -0.79$, $P = .004$).
- Neonates undergoing surgery on the 7th day of life had lower mean area under the flow curve values during both wash-in and washout (24 arbitrary units [au] $\times 10^3$ vs 92 au $\times 10^3$, $P = .02$) compared with neonates undergoing surgery before 7 days of life.

(8,9). Functional neuroimaging (eg, functional MRI) is technically challenging during ongoing neonatal cardiac surgery and therefore has limited capabilities for longitudinal intraoperative studies (10,11). US imaging has been recognized as a valuable tool with which to depict cerebral flow dynamics in infants (12). With the introduction of micron-size, gas-filled biodegradable shelled microbubbles used as vascular-specific US contrast agents, dynamic contrast-enhanced US has the capability to be used for quantitative perfusion imaging (13). Contrast-enhanced US has an excellent safety and pharmacologic profile, with liver and renal independent clearance (14). The U.S. Food and Drug Administration approved it for intravenous use for liver diagnostics in pediatric patients (15,16). This suggests that it is possible to perform intraoperative real-time transfontanellar neuroimaging studies with contrast-enhanced US (17,18). We hypothesized that transfontanellar contrast-enhanced US (T-CEUS) can depict and enable analysis of cerebral blood flow during neonatal ASO. Thus, we aimed to use T-CEUS to quantitatively assess cerebral perfusion in neonates undergoing ASO.

Materials and Methods

Study Design and Patients

Ethical and regulatory approval were obtained for this prospective single-center cross-sectional diagnostic trial. All parents or guardians gave written informed consent, and the trial was registered (ClinicalTrials.gov no. NCT03215628). Consecutive patients were recruited from February 2018 to February 2020 at the University Hospital Erlangen prior to individual surgical procedures. Infants aged 4 months or younger with TGA were eligible if they had a suitable imaging window (with open fontanel) and reasonable general health and neurologic status, and if a trained and certified physician qualified to perform the procedure was available. Neonates were excluded if this US physician was absent or if they had a known intolerance to

US contrast agents (or sulfur hexafluoride), poor general condition, or preexisting brain damage. For this study, one trial arm (neonates with TGA undergoing ASO) was analyzed. Data generated or analyzed during the study are available from the corresponding author by request.

Clinical Data

In all patients, continuous standard clinical monitoring was performed during the ASO procedure. Individual patient data before and during surgery were collected, including gestational week, age, weight, sex, heart rate, mean arterial pressure, central venous pressure, near-infrared spectroscopy findings, ventilation time, time spent in the pediatric intensive care unit, and total time in hospital. As part of standard monitoring, blood gas analyses (non-temperature-corrected analysis, α -stat method; temperature-corrected analysis, pH-stat method) were performed by a perfusionist (F.M., with 26 years of experience).

Imaging Studies

T-CEUS imaging was performed as described in previous studies (17). Briefly, a mobile high-end US system (Zonare ZS3, version 7.5; Shenzhen Mindray Bio-Medical Electronics) together with a curved array (Zonare C9-3 transducer; Shenzhen Mindray Bio-Medical Electronics) was used to perform imaging with the low-mechanical-index preset (mechanical index, 0.15). For all examinations, a trained and certified physician (J.J., with >20 years of experience in pediatric US) positioned the probe directly at the great fontanelle and kept a constant middle coronal plane during acquisition. For identification of clear visible anatomic landmarks and identification of both hemispheres, a middle coronal imaging plane was chosen. As reported before, the US contrast agent (0.04 mL per kilogram of body weight; SonoVue, Bracco) was injected intravenously as a bolus and was followed by a bolus of 2 mL 0.9% NaCl (17,19,20). While CPB was running, the US contrast agent dose was adjusted as follows: because blood volume in newborns is mostly calculated with approximately 85–100 mL/kg body weight (21) and the CPB was filled with a priming volume of 148 mL of blood, a compensation weight of 1 kg was added to the total body weight for contrast agent dose calculation. The mean absolute US contrast agent dose was 0.17 mL \pm 0.02 (SD), and mean weight-adapted US contrast agent doses were 0.04 mL/kg \pm 0.003 (no CPB, time points $T_1 + T_2$) and 0.05 mL/kg \pm 0.004 (CPB, time points $T_2 - T_3$), respectively.

Imaging Time Points

Imaging data were recorded at five different time points: before surgery (T_1), during high flow of the CPB at 37°C (T_2), during high flow of the CPB at 25°C–28°C (T_3), during low flow of the CPB at 25°C–28°C (T_4), and after surgery (T_5) (Fig 1A, 1B).

Software-based Analysis and Quantification

One investigator (F.K., with 11 years of experience in preclinical and clinical contrast-enhanced US) who did not perform or who was blinded to the results of intraoperative scanning had full access to all data and performed the independent analyses. Imaging data were exported as Digital Imaging and Communications in Medicine files, and quantification of time-intensity

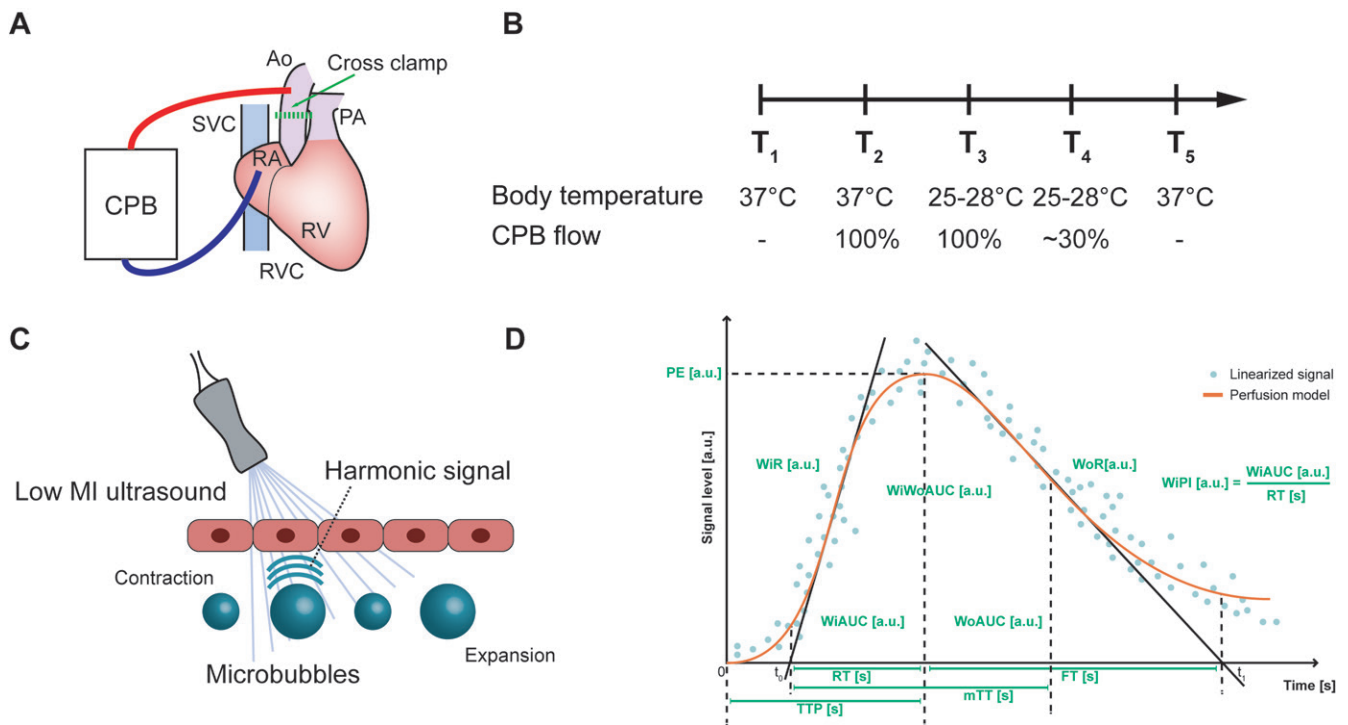


Figure 1: Study flow and technical approach. **(A)** Standardized routine arterial switch operation (ASO) was performed with a cardiopulmonary bypass (CPB). Ao = aorta, PA = pulmonary artery, RA = right atrium, RV = right ventricle, RVC = right vena cava, SVC = superior vena cava. **(B)** Imaging was performed at five time points during surgery (T_1 – T_5) at different body temperatures and under different CPB flow conditions. **(C)** In transfontanellar contrast-enhanced US, intravenous injected microbubbles were insonated, and signals were recorded as Digital Imaging and Communications in Medicine videos. **(D)** These videos were used for secondary software analysis to derive time-intensity curves for dynamic flow parameters. Imaging timepoints were as follows: T_1 = before surgery; T_2 = high CPB flow, 37°C; T_3 = high CPB flow, 25°C–28°C; T_4 = low CPB flow, 25°C–28°C; T_5 = end of surgery. FT = fall time, mTT = mean transit time, PE = peak enhancement, TTP = time-to-peak, WiAUC = area under the curve during wash-in, WiPI = wash-in perfusion index, WIR = wash-in rate, WIVoAUC = area under the curve during wash-in and washout, WoAUC = area under the curve during washout, WoR = washout rate, and RT = rise time.

Table 1: Assessed Parameters and Description for Transfontanellar Contrast-enhanced US

Parameter	Unit of Measure	Explanation
Peak enhancement	Arbitrary units	Maximum of signal intensity, peak signal level
AUC during wash-in	Arbitrary units	Integral from start (t_0) to peak, signal level of wash-in
Rise time	Seconds	Time from t_0 to peak, time for rise of signal level
Mean transit time	Seconds	Ratio of volume and flow
Time-to-peak	Seconds	Time to maximum signal, time for rise of signal level
Wash-in rate	Arbitrary units	Maximum slope ascending part
Wash-in perfusion index	Arbitrary units	AUC during wash-in divided by rise time
AUC during washout	Arbitrary units	Integral from peak to loss of signal (t_1), signal level of washout
AUC during wash-in and washout	Arbitrary units	AUC during wash-in and AUC during washout, total signal level
Fall time	Seconds	t_1 time-to-peak
Wash-out rate	Arbitrary units	Minimum slope descending part

Note.—AUC = area under the curve, t_0 = time point for first detection of signal, t_1 = time point for loss of signal.

curves was performed with dedicated software (VueBox, version 7.1.5.58024; Bracco Suisse). The software enables generation of time-intensity curves from recorded T-CEUS scans as surrogates of microbubble flow over time in a predefined region of interest (22,23). For the secondary software-based analyses, signals were measured in both cerebral hemispheres (right and left) and in the superior sagittal sinus (venous). For all measurements, the manufacturer provided a calibration file specified for the used

US device and imaging probe. As a result, 11 dynamic flow parameters were generated for subsequent analyses (Table 1). Figure 1C and 1D describes the approach from intravenous injection to generation of T-CEUS parameters. Table 1 summarizes the assessed parameters and gives their description. For the final analysis, a total of 60 investigations were included. If single parameters could not be calculated, then these data points were excluded from the final analysis.

Statistical Analyses

Because no prior data were available, no power calculation was performed. The sample size of 12 neonates was deemed ethically justified for this study. Data are given as mean ± SD. Statistical analysis was performed with GraphPad Prism (version 9.0; GraphPad). Normal distribution of values was tested with the Shapiro-Wilk test and inspected with quantile-quantile plots. Differences of signal level in relation to baseline were tested with repeated measures two-way analysis of variance and the Dunnett multiple comparisons test. In case of missing values, a mixed-effects model was used. A comparison of two groups was performed with a two-tailed unpaired *t* test. For correlation matrices, T-CEUS parameters of the right hemisphere at every surgical step were correlated with age at surgery. Coefficients are reported as Pearson correlation coefficients. *P* < .05 was considered indicative of a significant difference. For age group analyses, the study sample was empirically divided into young (<7 days) and old (≥7 days) patients based on time to surgery (six patients per group). A receiver operating characteristic curve was used to describe the relationship between sensitivity and specificity at different thresholds.

Results

Neonate Characteristics

A total of 22 neonates were screened for inclusion. Four neonates were excluded due to their unstable general condition, and six were excluded because the parents did not give consent for the study or the imaging physician was unavailable.

Finally, 12 neonates with a mean gestational age of 39 6/7 weeks ± 1/7 were included in the final analysis (Fig 2). They underwent ASO a mean of 6.9 days ± 3.4 (range, 2–16 days) after birth. There was no associated mortality, and all neonates were discharged alive. Two neonates experienced infectious episodes, and one neonate had low cardiac output and underwent extracorporeal membrane oxygenation and dialysis after completion of ASO. In one neonate, microcephaly was noticed without any other signs of syndromic disease. Median head circumference was 34.7 cm ± 1.3. Demographic data of the neonates are summarized in Table 2.

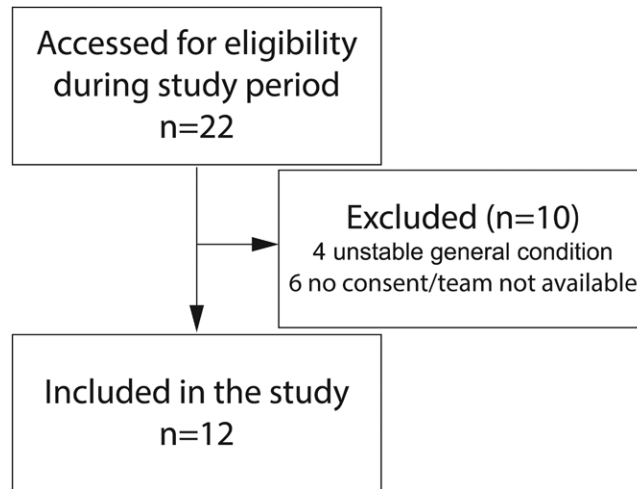


Figure 2: Study flowchart.

Table 2: Characteristics of Neonates Undergoing ASO

Participant No.	Diagnosis	Underwent Rashkind Procedure	PG	No. of Gestational Weeks	Weight (kg)	Age at Surgery (d)	Head Circumference (cm)	In-house Delivery	Coronary Artery Patterns	Other
1	D-TGA, VSD	Y	Y	41 4/7	4.10	5	38.0	N	1: L; 2: R, Cx	NA
2	D-TGA	Y	Y	41 3/7	3.70	10	35.0	N	1: L, Cx; 2: R	NA
3	D-TGA	N	Y	39 6/7	3.50	5	34.0	Y	1: L; 2: R, Cx	NA
4	D-TGA	Y	Y	41 4/7	3.60	7	35.0	Y	1: L, Cx; 2: R	NA
5	D-TGA	N	Y	40 2/7	3.96	16	34.0	Y	1: L, Cx; 2: R	Postoperative sepsis
6	D-TGA	N	Y	39 2/7	2.80	5	32.5	N	1: L; 2: R, Cx	Microcephaly
7	D-TGA	Y	Y	39 5/7	3.60	2	34.5	N	1: L, Cx; 2: R	NA
8	D-TGA, VSD	Y	Y	38 1/7	3.45	7	34.0	N	1: L; 2: R, Cx	NA
9	D-TGA	N	Y	38 2/7	3.80	6	34.0	N	1: L, Cx; 2: R	NA
10	D-TGA	Y	Y	41 0/7	3.80	7	35.5	N	1: L, Cx; 2: R	NA
11	D-TGA	Y	Y	37 2/7	2.70	7	34.5	Y	1: L; 2: R, Cx	Postoperative ECMO, dialysis
12	D-TGA, VSD	Y	Y	40 4/7	3.40	6	35.5	N	1: L, Cx; 2: R	Postoperative, SIRS
Mean ± SD	NA	NA	NA	39 6/7 ± 1/7	3.5 ± 0.4	6.9 ± 3.4	34.7 ± 1.3	NA	NA	NA

Note.—ASO = arterial switch operation, Cx = circumflex artery, D-TGA = dextro-transposition of the great arteries, ECMO = extracorporeal membrane oxygenation, L = left coronary artery, N = no, NA = not applicable, PG = prostaglandin infusion, R = right coronary artery, SIRS = systemic inflammatory response syndrome, VSD = ventricle septum defect, Y = yes.

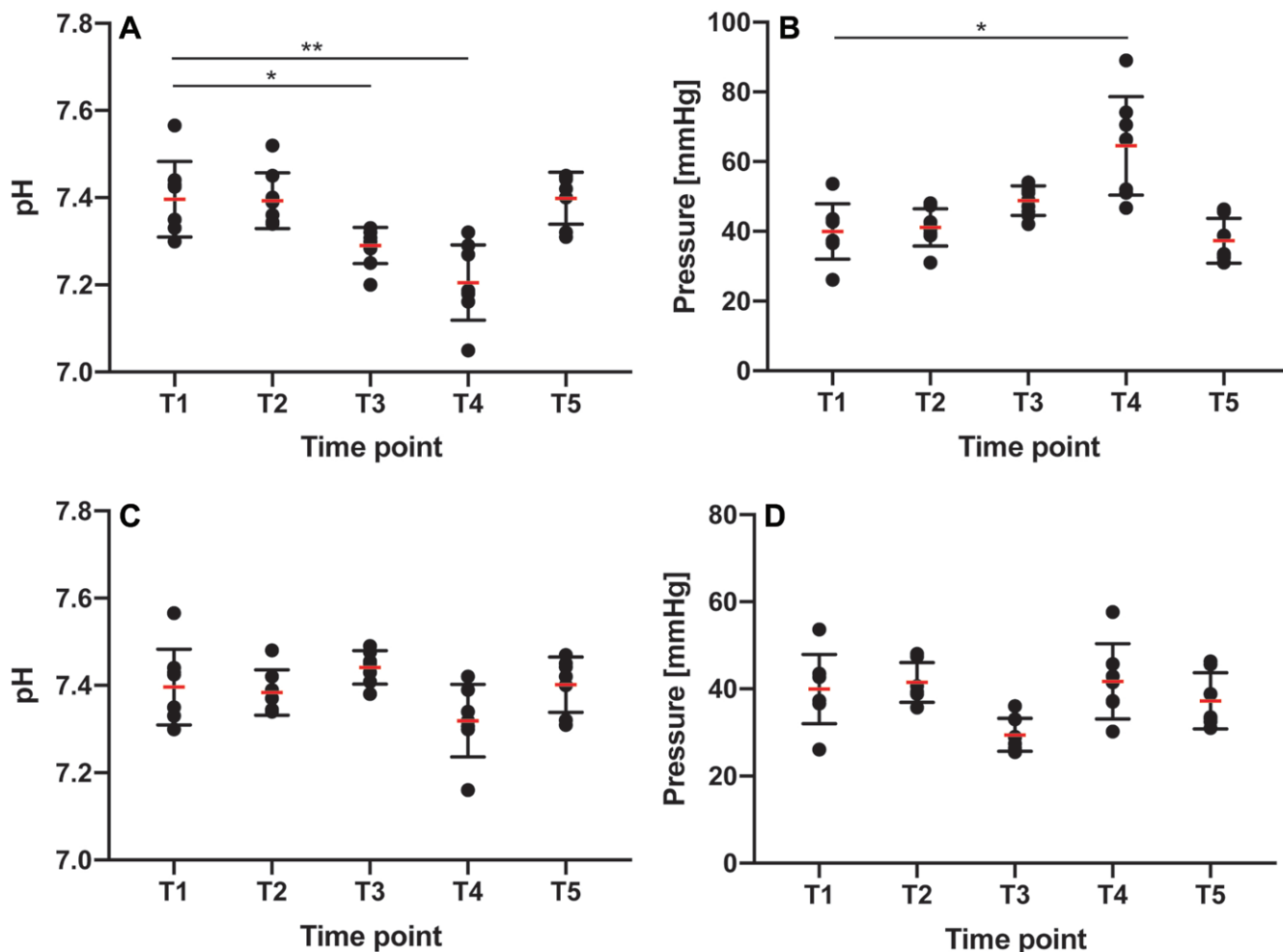


Figure 3: Box and whisker plots show blood gas samples obtained during arterial switch operation. Horizontal lines indicate the mean, and lower and upper bars indicate SD. During the intervention, **(A)** pH (α -stat method) decreased and **(B)** partial pressure of carbon dioxide (P_{CO_2}) increased significantly. After temperature correction (pH-stat method), values for **(C)** pH and **(D)** P_{CO_2} showed no significant changes. * = $P < .05$, ** = $P < .01$.

Clinical Parameters during ASO

Mean radial blood pressure was $41 \text{ mmHg} \pm 6.8$ at baseline (T_1) and $48 \text{ mmHg} \pm 13$ at T_2 ($P = .41$), $39 \text{ mmHg} \pm 13$ at T_3 ($P = .95$), $29 \text{ mmHg} \pm 12$ at T_4 ($P = .026$), and $55 \text{ mmHg} \pm 8.1$ at T_5 ($P < .001$) (Fig 3A). As a result of the reconstruction of a physiologic cardiovascular anatomy, regional cerebral oxygenation level of the lower body as measured with near-infrared spectroscopy increased from $44\% \pm 16$ at T_1 to $53\% \pm 22$ at T_2 ($P = .10$), $67\% \pm 19$ at T_3 ($P = .008$), $62\% \pm 16$ at T_4 ($P = .002$), and a postoperative peak of $76\% \pm 11$ at T_5 ($P < .001$) (Fig 3B). Regional cerebral oxygenation level measured in the bilateral cerebral hemispheres remained within the normal range during the entire course of ASO (Fig 3C, 3D).

As measured with the α -stat method, pH decreased, and partial pressure of carbon dioxide (P_{CO_2}) increased at T_4 when compared with baseline levels. In arterial blood samples, pH was 7.4 ± 0.1 at T_1 , 7.4 ± 0.1 at T_2 ($P > .99$), 7.3 ± 0.04 at T_3 ($P = .048$), 7.2 ± 0.1 at T_4 ($P = .009$), and 7.4 ± 0.1 at T_5 ($P > .99$) and P_{CO_2} was $40 \text{ mmHg} \pm 7.9$ at T_1 , $41 \text{ mmHg} \pm 5.4$ at T_2 ($P = .98$), $49 \text{ mmHg} \pm 4.3$ at T_3 ($P = .10$), $65 \text{ mmHg} \pm 14$ at T_4 ($P = .014$), and $37 \text{ mmHg} \pm 6.4$ at T_5 ($P = .67$) (Fig 4A, 4B). As measured

with the temperature-corrected pH-stat method, pH and P_{CO_2} remained unchanged when compared with baseline values. The pH was 7.4 ± 0.1 at T_1 , 7.4 ± 0.1 at T_2 ($P = .89$), 7.4 ± 0.04 at T_3 ($P = .60$), 7.3 ± 0.1 at T_4 ($P = .33$), and 7.40 ± 0.06 at T_5 ($P > .99$), and P_{CO_2} was $40 \text{ mmHg} \pm 7.9$ at T_1 , $41 \text{ mmHg} \pm 4.6$ at T_2 ($P = .86$), $29 \text{ mmHg} \pm 3.8$ at T_3 ($P = .13$), $42 \text{ mmHg} \pm 8.6$ at T_4 ($P = .86$), and $37 \text{ mmHg} \pm 6.4$ at T_5 ($P = .68$) (Fig 4C, 4D).

Cerebral Perfusion during ASO

Dynamic flow parameters were analyzed during the course of ASO, and secondary analyses of captured T-CEUS scans revealed changes associated with each surgical step (Fig 5A, Movie 1 [online]). When plotting individual time-intensity curves, a marked change in the slope of the curves was noticed, especially during T_4 (Fig 5B). When compared with the baseline measurement, the quantitative analyses showed a longer mean time-to-peak in the right hemisphere from $4.3 \text{ seconds} \pm 2.1$ at T_1 to $8.3 \text{ seconds} \pm 5.2$ at T_2 ($P = .10$), $9.1 \text{ seconds} \pm 4.3$ at T_3 ($P = .024$), and $17 \text{ seconds} \pm 6.4$ at T_4 ($P < .001$) during low-flow CPB and hypothermia. After ASO, mean time-to-peak normalized to $5.1 \text{ seconds} \pm$

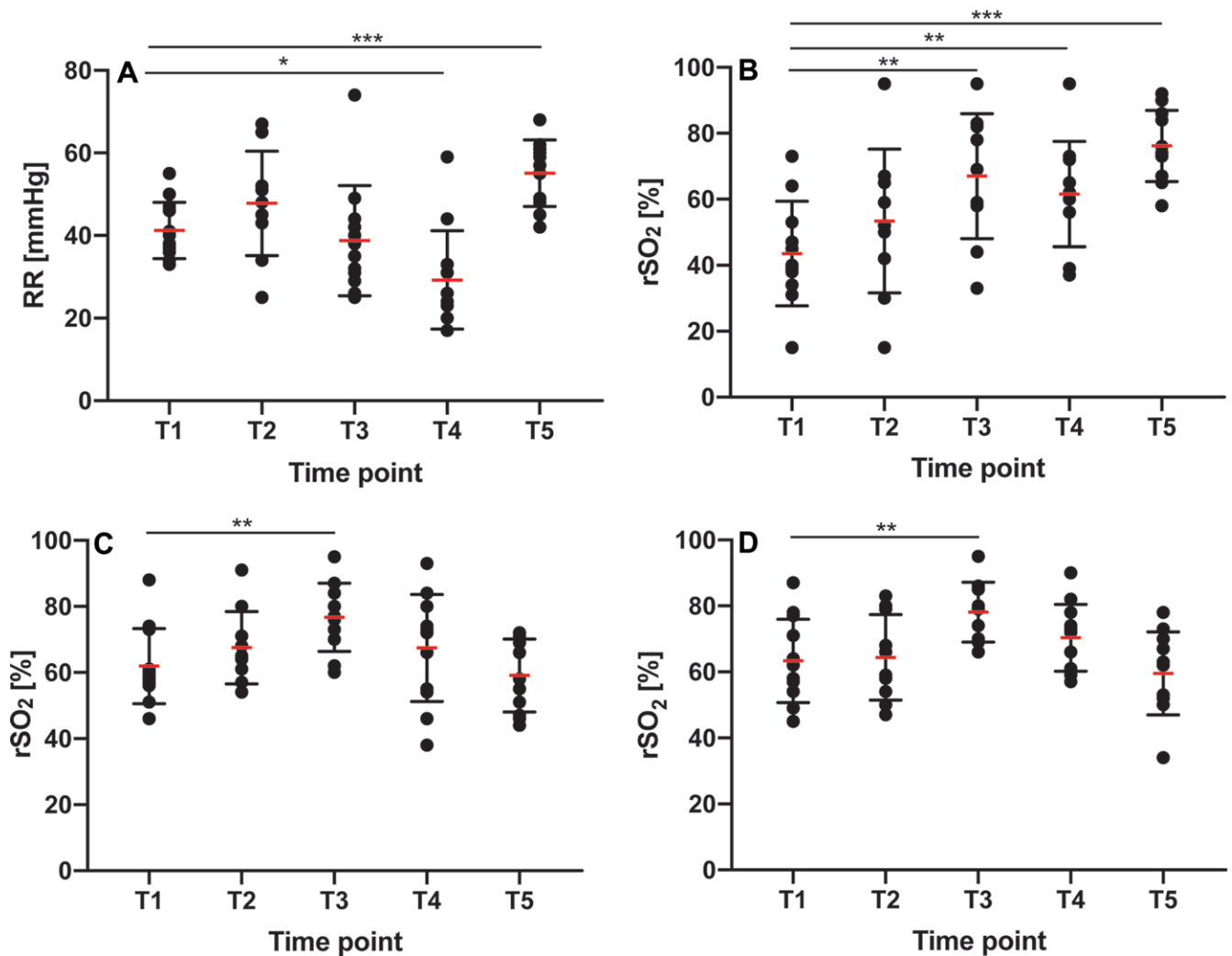


Figure 4: Box and whisker plots show radial artery blood pressure and near-infrared spectroscopy (NIRS) measurements obtained during an arterial switch operation (ASO). Horizontal lines indicate the mean, and lower and upper bars indicate SD. **(A)** During the intervention, radial blood pressure was significantly lowered. **(B)** NIRS measurements of the lower body relative cerebral oxygenation level increased after ASO, while values were normal in the individual hemispheres **(C, D)**. * = $P < .05$, ** = $P < .01$, *** = $P < .001$.

2.2 (T_5 , $P = .73$). In the left hemisphere, mean time-to-peak also increased from 4.0 seconds \pm 2.3 at T_1 to 11 seconds \pm 9.8 at T_2 ($P = .12$), 8.4 seconds \pm 2.6 at T_3 ($P = .001$), 21 seconds \pm 8.7 at T_4 ($P < .001$), and 5.4 seconds \pm 1.6 at T_5 ($P = .41$). Similar increases were also seen for rise time in both cerebral hemispheres (Fig 5C). All quantitative T-CEUS parameters for measurement of both cerebral hemispheres are presented in Tables E1 and E2 (online) and Figures E1 and E2 (online). The T-CEUS parameters in the superior sagittal sinus remained unchanged and are given in Tables E3 and E4 (online).

Association of Imaging and Age

A negative correlation of neonate age and T-CEUS flow parameters in the right cerebral hemisphere during T_4 of ASO was found for area under the flow curve (AUC) during wash-in ($r = -0.69$, $P = .020$), washout ($r = -0.82$, $P = .002$), and both wash-in and washout ($r = -0.79$, $P = .004$). We did not find a correlation between age at surgery and the other recorded clinical parameters (Fig 6A; Fig E3 [online]).

When dividing our sample into neonates undergoing surgery before 7 days (<7 days, $n = 6$) and on day 7 or after (≥ 7 days, $n = 6$), differences in AUC during wash-in, washout, and both wash-in and washout were visible on color-coded perfusion maps (Fig 6B; Movie 2 [online]). During surgical step T_4 , CPB flow was reduced, which was not related to the age of the neonate and which did not differ between the two subgroups (Fig 6C).

AUCs during wash-in ($[87 \text{ arbitrary units } \{au\} \pm 77] \times 10^2$ vs $[270 \text{ au} \pm 164] \times 10^2$, $P = .049$), during washout ($[15 \text{ au} \pm 11] \times 10^3$ vs $[65 \text{ au} \pm 38] \times 10^3$, $P = .020$), and during both ($[24 \text{ au} \pm 18] \times 10^3$ vs $[92 \text{ au} \pm 53] \times 10^3$, $P = .023$) were lower in neonates 7 days or older at surgery than in younger neonates (Fig 5D). Given a cutoff of $47 \text{ au} \times 10^3$ for AUC during wash-in and washout, receiver operating characteristic analysis showed a sensitivity of 100% (12 of 12) and a specificity of 67% (eight of 12) (AUC, 0.93; 95% CI: 0.78, 1.00; $P < .018$) in the discrimination of younger from older neonates (Fig E4 [online]). In contrast, we found no difference in timing of surgical procedures between these groups (eg, time between T_1 and T_5 in younger vs

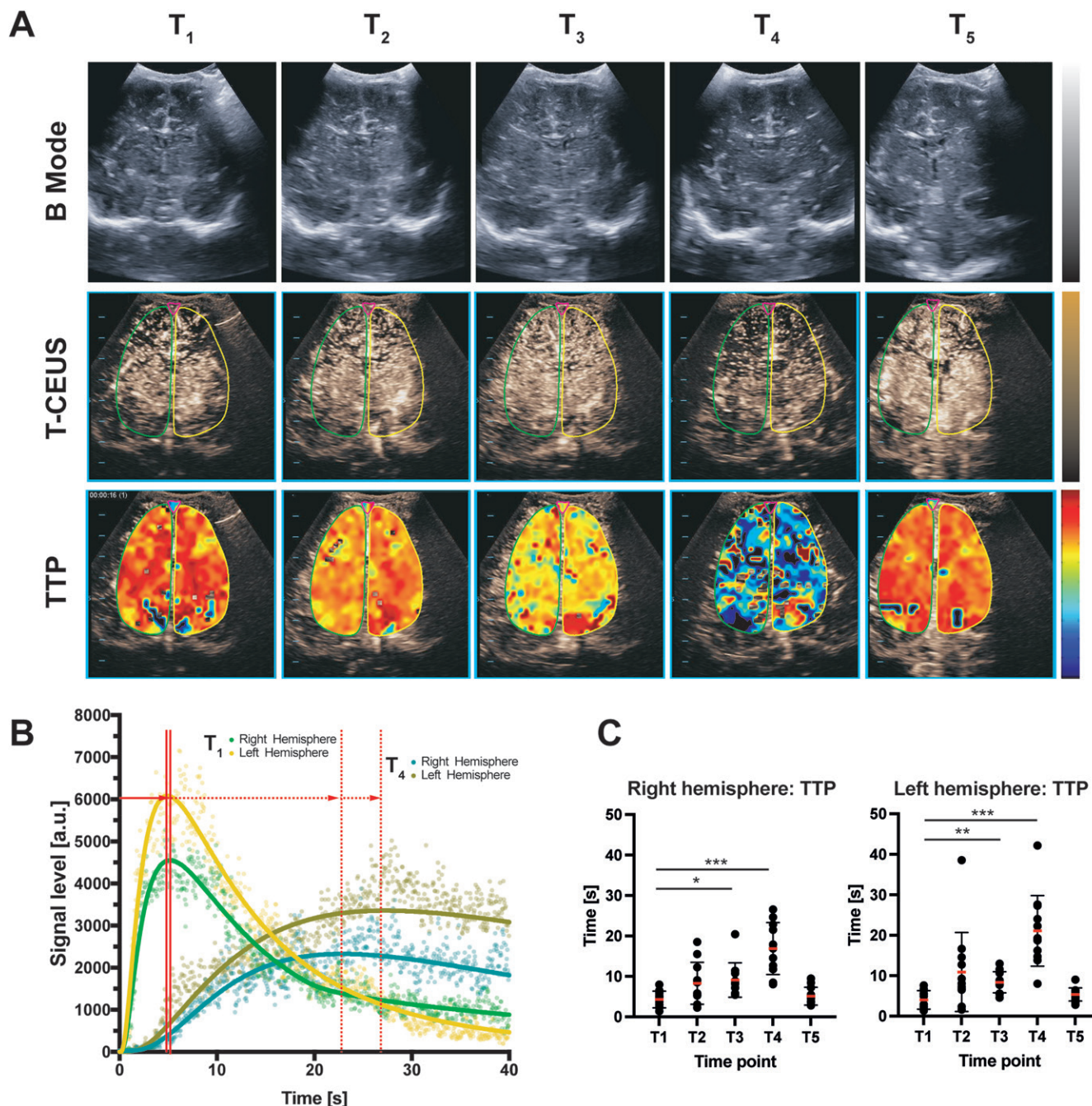


Figure 5: Images show changes in perfusion during arterial switch operation (ASO). **(A)** A marked decrease in cerebral perfusion was found during T_4 (low cardiopulmonary bypass [CPB] flow, hypothermia). **(B, C)** Transfontanellar contrast-enhanced US (T-CEUS) time-intensity curves showed altered flow profile from T_1 (before surgery) compared with T_4 (low CPB flow, hypothermia) **(B)**, with delayed influx of microbubbles resulting in a longer time-to-peak (TTP) **(C)** as indicated by the solid (T_1) and dashed red lines and arrow (T_3 , end of surgery). $** = P < .01$, $*** = P < .001$. Imaging timepoints: T_1 = before surgery; T_2 = high CPB flow, 37°C ; T_3 = high CPB flow, $25\text{--}28^\circ\text{C}$; T_4 = low CPB flow, $25\text{--}28^\circ\text{C}$; T_5 = end of surgery.

older neonates: 5 hours 11 minutes \pm 57 minutes 7 seconds vs 5 hours 35 minutes \pm 28 minutes 52 seconds; $P = .42$) (Table E5 [online]).

Discussion

Monitoring of cerebral blood flow during cardiac surgery in infants with congenital heart disease is particularly important. In this prospective trial of 12 neonates undergoing neonatal heart surgery, we used transfontanellar contrast-enhanced US

(T-CEUS) to perform intraoperative real-time cerebral perfusion imaging. We found a significant reduction in cerebral perfusion associated with low-flow cardiopulmonary bypass (CPB) and lower body temperature—both of which are essential components of standard arterial switch operation procedures. This was demonstrated by an increase in the mean time-to-peak value in the right hemisphere from 4.3 seconds \pm 2.1 at T_1 to 8.3 seconds \pm 5.2 at T_2 , ($P = .10$), 9.1 seconds \pm 4.3 at T_3 ($P = .024$), and 17 seconds \pm 6.4 at T_4 ($P < .001$) during low-flow CPB and hypo-

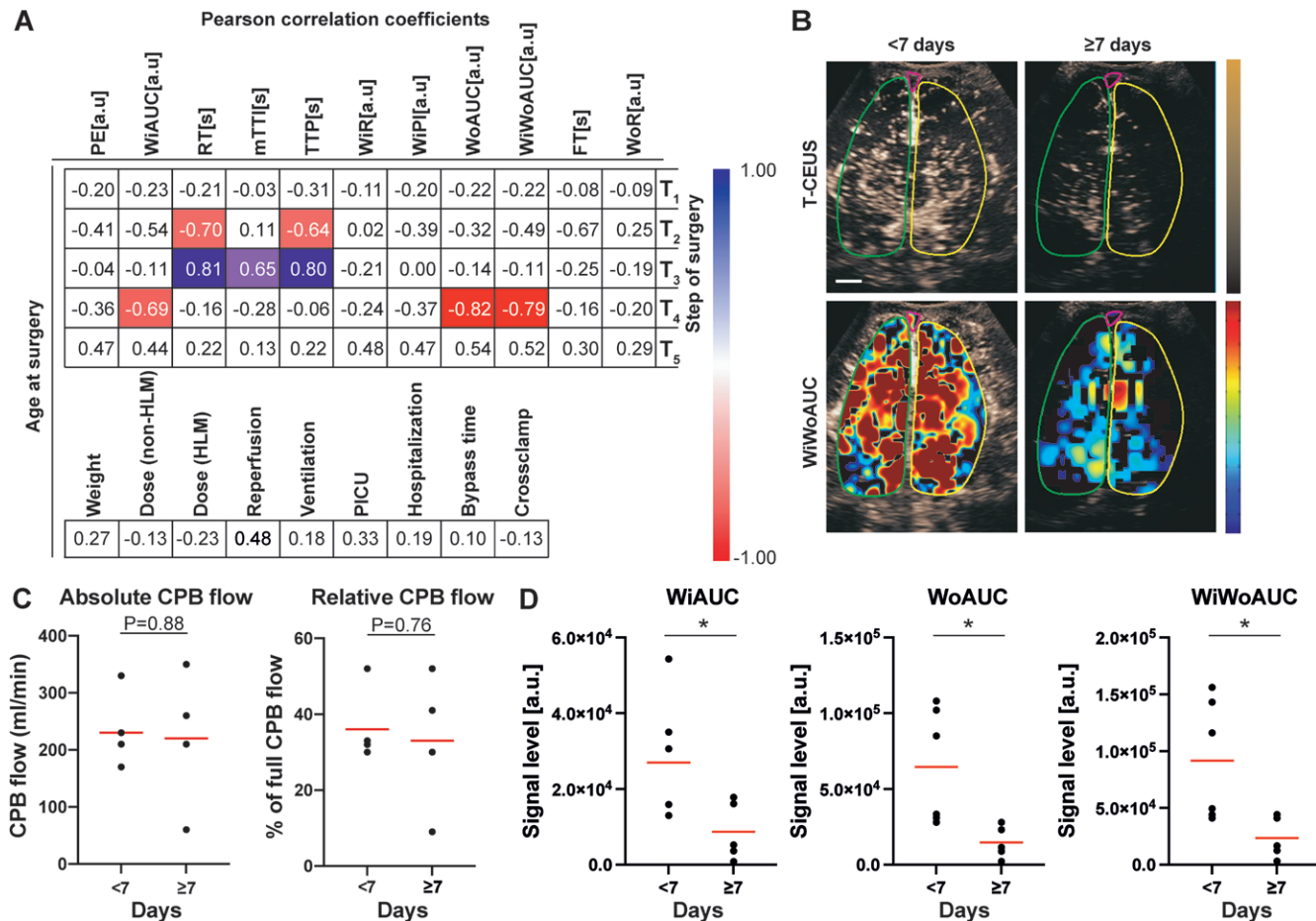


Figure 6: Changes of perfusion during transposition of the great arteries (TGA) surgery with cardiopulmonary bypass (CPB). Pearson correlation matrix of the individual age at surgery at the different surgical steps (T_1 – T_5) and all transfontanellar contrast-enhanced US (T-CEUS) parameters. A negative correlation of cerebral perfusion and age was found in surgical step T_4 (low flow, hypothermia). **(A)** Significant values are colored. **(B)** When dividing the entire study sample in neonates receiving surgery early (<7 days of life) versus late (≥ 7 days of life), the difference could also be seen with T-CEUS. **(C)** While the subgroups demonstrated no difference in absolute or relative CPB flow, **(D)** they showed significant differences in the T-CEUS parameters area under the flow curve (AUC) during wash-in (WiAUC), AUC during wash-out (WoAUC), and AUC during wash-in and washout (WiWoAUC). $*$ = $P < .05$. Imaging time points: T_1 = before surgery; T_2 = high CPB flow, 37°C; T_3 = high CPB flow, 25–28°C; T_4 = low CPB flow, 25–28°C; T_5 = end of surgery.

thermia. These effects were only transitory and disappeared after completion of surgery (5.1 seconds \pm 2.2 at T_5 [$P = .73$]) and re-establishment of normal circulatory conditions. At low-flow CPB and lower body temperature, neonate age at surgery negatively correlated with T-CEUS flow parameters as indicated by the area under the flow curve (AUC) during wash-in ($r = -0.69$, $P = .020$), washout ($r = -0.82$, $P = .002$), and both wash-in and washout ($r = -0.79$, $P = .004$). AUC values were lower in neonates 7 days or older at the time of surgery compared with younger neonates during wash-in ($[87 \text{ au} \pm 77] \times 10^2$ vs $[270 \text{ au} \pm 164] \times 10^2$, $P = .049$), during washout ($[15 \text{ au} \pm 11] \times 10^3$ vs $[65 \text{ au} \pm 38] \times 10^3$, $P = .020$) and during both wash-in and washout ($[24 \text{ au} \pm 18] \times 10^3$ vs $[92 \text{ au} \pm 53] \times 10^3$, $P = .023$).

Impaired cerebral circulation and hypoxia negatively impact neuroanatomic and developmental outcomes in those with congenital heart disease (24,25). Although unproven, there is growing evidence that earlier repair in transposition of the great arteries is beneficial (5,26), especially in terms of lower health care costs, morbidity, and neurodevelopmental outcomes (27,28). In physiologic conditions, P_{CO_2} increases and partial pressure of oxygen decreases during advancement

of pregnancy (29,30). However, MRI revealed a more pronounced increased cerebral hypoxia in fetuses (31) and newborns (32) with complex congenital heart disease. On a molecular level, this hypoxic state, especially when persistent after delivery, might enhance abnormal neuronal proliferation (33) and alter cerebral vasculature (34). This leads to phenotypic de-differentiation of cerebrovascular smooth muscle cells and results in a loss of contractile capacity and physiologic adaption mechanisms (35). Chronic hypoxia, as is also seen in intrauterine growth restriction, is correlated with lower vascular density, lower endothelial cell proliferation, and reduced pericyte and astrocyte attachment (36). These mechanisms might explain why the cerebral vasculature of older neonates, who experienced relative hypoxia for a longer time, may be less responsive to vasodilatory stimuli (37). These transient effects, as depicted with T-CEUS, could possibly be enhanced by the more unfavorable physiologic conditions (lower blood pressure, lower pH, and higher P_{CO_2}) during low-flow CPB.

To date, US imaging has been widely used to depict cerebral blood flow in neonates (12). Color duplex US of the

extracranial cerebral arteries can be used to measure volume of global cerebral blood flow in healthy preterm and term neonates (38). Transfontanellar and transtemporal two- and three-dimensional power and color Doppler US can depict cerebral blood flow intensity in the main cerebral vessels (39). For this, time average velocities can be measured with combined pulse-wave Doppler US (9). When compared with T-CEUS, these techniques are unable to quantitatively depict perfusion in brain parenchyma. T-CEUS allows analysis of dynamic flow parameters as surrogates for tissue perfusion (22,40). Whereas the US contrast agent is cleared for intravascular applications, intravenous administration in pediatric patients is an off-label use in Europe (19).

Our study had limitations. First, our study was limited by its small sample size and clinically heterogeneous study sample. Second, small fontanelles constrained not only the accessibility or field of view to the central nervous system of the newborn, but also the available space to place the US probe during surgery. The central and symmetric positioning of the US probe and the reduction of movements are essential quality parameters for transfontanellar US. Third, the image quality could have been influenced by electric disturbances like electrocautery or the cardiac output (CO), a product of stroke volume (SV) and heart rate (HR) ($CO = SV \times HR$), which can be especially variable in children. Fourth, compared with other techniques such as near-infrared spectroscopy, transfontanellar contrast-enhanced US cannot be used as a method for continuous monitoring during the entire surgery.

In conclusion, our study revealed quantitative age-dependent brain perfusion patterns during arterial switch operation (ASO). Although the technique requires further validation with larger sample sizes and correlation with clinical parameters and outcome measures, the findings provide insight into intraoperative cerebral circulation and may support earlier ASO in neonates with transposition of the great arteries.

Acknowledgment: We thank Bracco Suisse for providing the software calibration file used for quantification software.

Author contributions: Guarantors of integrity of entire study, **E.K., R.C., A.R.**; study concepts/study design or data acquisition or data analysis/interpretation, all authors; manuscript drafting or manuscript revision for important intellectual content, all authors; approval of final version of submitted manuscript, all authors; agrees to ensure any questions related to the work are appropriately resolved, all authors; literature research, **E.K., R.C., A.L.W., S.D., J.J.**; clinical studies, **E.K., R.C., A.P., F.M., A.N., J.J., A.R.**; statistical analysis, **E.K., R.C.**; and manuscript editing, **E.K., R.C., A.P.R., A.L.W., S.D., F.M., J.W., J.J., A.R.**

Data sharing. Data generated or analyzed during the study are available from the corresponding author by request.

Disclosures of conflicts of interest: **E.K.** No relevant relationships. **R.C.** Ake Senning lecture (Zurich, Germany; October 7, 2021), Pediatric Update (Zurich, Germany; October 27, 2021), and DGPk Webinar HLHS (November 6, 2020); leadership role in the German Society for Thoracic and Cardiovascular Surgery and European Association for Cardio-Thoracic Surgery. **A.P.R.** No relevant relationships. **A.L.W.** No relevant relationships. **A.P.** No relevant relationships. **S.D.** Institutional research contract with Siemens; presentation for Corlife at the presentation at the Deutsche Gesellschaft für Pädiatrische Kardiologie e.V. Congress 2021; advisory board of the BeGrow study for Bentley Innomed; steering committee for the German Society for Pediatric Cardiology and Congenital Heart Disease. **F.M.** Consulting fees from Lauda Medical Pfarrstraße; presentations for CytoSorbents

Europe. **A.N.** Grants from the German Ministry of Health and European Commission Innovation Fond of the Joint Federal Committee. **J.W.** Consulting fees from Ipsen, Hexal, and Novo Nordisk; lecture fees from Pfizer, Merck, and Novo Nordisk; board member of patient support group Bundesverband Kleinwüchsige Menschen und ihre Familien e.V. and German Society of Pediatric Endocrinology and Diabetology. **J.J.** No relevant relationships. **A.R.** No relevant relationships.

References

- Moons P, Bovijn L, Budts W, Belmans A, Gewillig M. Temporal trends in survival to adulthood among patients born with congenital heart disease from 1970 to 1992 in Belgium. *Circulation* 2010;122(22):2264–2272.
- Raissadati A, Nieminen H, Haukka J, Sairanen H, Jokinen E. Late Causes of Death After Pediatric Cardiac Surgery: A 60-Year Population-Based Study. *J Am Coll Cardiol* 2016;68(5):487–498.
- Marathe SP, Talwar S. Surgery for transposition of great arteries: A historical perspective. *Ann Pediatr Cardiol* 2015;8(2):122–128.
- Best KE, Rankin J. Long-Term Survival of Individuals Born With Congenital Heart Disease: A Systematic Review and Meta-Analysis. *J Am Heart Assoc* 2016;5(6):e002846.
- Petit CJ, Rome JJ, Wernovsky G, et al. Preoperative brain injury in transposition of the great arteries is associated with oxygenation and time to surgery, not balloon atrial septostomy. *Circulation* 2009;119(5):709–716.
- Newburger JW, Jonas RA, Wernovsky G, et al. A comparison of the perioperative neurologic effects of hypothermic circulatory arrest versus low-flow cardiopulmonary bypass in infant heart surgery. *N Engl J Med* 1993;329(15):1057–1064.
- Bellinger DC, Wypij D, duPlessis AJ, et al. Neurodevelopmental status at eight years in children with dextro-transposition of the great arteries: the Boston Circulatory Arrest Trial. *J Thorac Cardiovasc Surg* 2003;126(5):1385–1396.
- von Rhein M, Buchmann A, Hagmann C, et al. Brain volumes predict neurodevelopment in adolescents after surgery for congenital heart disease. *Brain* 2014;137(Pt 1):268–276.
- Rüffer A, Tischer P, Münch F, et al. Comparable Cerebral Blood Flow in Both Hemispheres During Regional Cerebral Perfusion in Infant Aortic Arch Surgery. *Ann Thorac Surg* 2017;103(1):178–185.
- Mahle WT, Tavani F, Zimmerman RA, et al. An MRI study of neurological injury before and after congenital heart surgery. *Circulation* 2002;106(12 Suppl 1):I109–I114.
- McQuillen PS. Magnetic resonance imaging in congenital heart disease: what to do with what we see and don't see? *Circulation* 2009;119(5):660–662.
- Archer LN, Levene MI, Evans DH. Cerebral artery Doppler ultrasonography for prediction of outcome after perinatal asphyxia. *Lancet* 1986;2(8516):1116–1118.
- Rafailidis V, Deganello A, Watson T, Sidhu PS, Sellars ME. Enhancing the role of paediatric ultrasound with microbubbles: a review of intravenous applications. *Br J Radiol* 2017;90(1069):20160556.
- Morel DR, Schwieger I, Hohn L, et al. Human pharmacokinetics and safety evaluation of SonoVue, a new contrast agent for ultrasound imaging. *Invest Radiol* 2000;35(1):80–85.
- Seitz K, Strobel D. A Milestone: Approval of CEUS for Diagnostic Liver Imaging in Adults and Children in the USA. *Ultraschall Med* 2016;37(3):229–232.
- Dietrich CF, Augustiniene R, Batko T, et al. European Federation of Societies for Ultrasound in Medicine and Biology (EFSUMB): An Update on the Pediatric CEUS Registry on Behalf of the “EFSUMB Pediatric CEUS Registry Working Group”. *Ultraschall Med* 2021;42(3):270–277.
- Knieling F, Rüffer A, Cesnjevar R, et al. Transfontanellar Contrast-Enhanced Ultrasound for Monitoring Brain Perfusion During Neonatal Heart Surgery. *Circ Cardiovasc Imaging* 2020;13(3):e010073.
- Hwang M, Barnewolt CE, Jüngert J, Prada F, Sridharan A, Didier RA. Contrast-enhanced ultrasound of the pediatric brain. *Pediatr Radiol* 2021;51(12):2270–2283.
- Knieling F, Strobel D, Rompel O, et al. Spectrum, Applicability and Diagnostic Capacity of Contrast-Enhanced Ultrasound in Pediatric Patients and Young Adults after Intravenous Application - A Retrospective Trial. *Ultraschall Med* 2016;37(6):619–626.
- Rüffer A, Knieling F, Cesnjevar R, et al. Equal cerebral perfusion during extended aortic coarctation repair. *Eur J Cardiothorac Surg* 2022;61(2):299–306.
- Duke T, Molyneux EM. Intravenous fluids for seriously ill children: time to reconsider. *Lancet* 2003;362(9392):1320–1323.
- Lassau N, Koscielny S, Chami L, et al. Advanced hepatocellular carcinoma: early evaluation of response to bevacizumab therapy at dynamic

- contrast-enhanced US with quantification--preliminary results. *Radiology* 2011;258(1):291-300.
23. Knieling F, Waldner MJ, Goertz RS, Strobel D. Quantification of dynamic contrast-enhanced ultrasound in HCC: prediction of response to a new combination therapy of sorafenib and panobinostat in advanced hepatocellular carcinoma. *BMJ Case Rep* 2012;2012:bcr2012007576.
 24. Ibuki K, Watanabe K, Yoshimura N, et al. The improvement of hypoxia correlates with neuroanatomic and developmental outcomes: comparison of midterm outcomes in infants with transposition of the great arteries or single-ventricle physiology. *J Thorac Cardiovasc Surg* 2012;143(5):1077-1085.
 25. Miller SP, McQuillen PS, Hamrick S, et al. Abnormal brain development in newborns with congenital heart disease. *N Engl J Med* 2007;357(19):1928-1938.
 26. Rollins CK, Newburger JW. Correction of d-Transposition of the Great Arteries Sooner Rather Than Later. *Circulation* 2019;139(24):2739-2741.
 27. Anderson BR, Ciarleglio AJ, Hayes DA, Quaegebeur JM, Vincent JA, Bacha EA. Earlier arterial switch operation improves outcomes and reduces costs for neonates with transposition of the great arteries. *J Am Coll Cardiol* 2014;63(5):481-487.
 28. Lim JM, Porayette P, Marini D, et al. Associations Between Age at Arterial Switch Operation, Brain Growth, and Development in Infants With Transposition of the Great Arteries. *Circulation* 2019;139(24):2728-2738.
 29. Soothill PW, Nicolaides KH, Rodeck CH, Campbell S. Effect of gestational age on fetal and intervillous blood gas and acid-base values in human pregnancy. *Fetal Ther* 1986;1(4):168-175.
 30. Sinding M, Peters DA, Frøkjær JB, et al. Placental magnetic resonance imaging T2* measurements in normal pregnancies and in those complicated by fetal growth restriction. *Ultrasound Obstet Gynecol* 2016;47(6):748-754.
 31. Lauridsen MH, Ulbjerg N, Henriksen TB, et al. Cerebral Oxygenation Measurements by Magnetic Resonance Imaging in Fetuses With and Without Heart Defects. *Circ Cardiovasc Imaging* 2017;10(11):e006459.
 32. Lim JM, Kingdom T, Saini B, et al. Cerebral oxygen delivery is reduced in newborns with congenital heart disease. *J Thorac Cardiovasc Surg* 2016;152(4):1095-1103.
 33. Morton PD, Korotcova L, Lewis BK, et al. Abnormal neurogenesis and cortical growth in congenital heart disease. *Sci Transl Med* 2017;9(374):eaah7029.
 34. Verma RK, Keller D, Grunt S, et al. Decreased oxygen saturation levels in neonates with transposition of great arteries: Impact on appearance of cerebral veins in susceptibility-weighted imaging. *Sci Rep* 2017;7(1):15471.
 35. Pearce WJ. Fetal Cerebrovascular Maturation: Effects of Hypoxia. *Semin Pediatr Neurol* 2018;28:17-28.
 36. Castillo-Melendez M, Yawno T, Allison BJ, Jenkin G, Wallace EM, Miller SL. Cerebrovascular adaptations to chronic hypoxia in the growth restricted lamb. *Int J Dev Neurosci* 2015;45(1):55-65.
 37. Kooi EMW, Richter AE. Cerebral Autoregulation in Sick Infants: Current Insights. *Clin Perinatol* 2020;47(3):449-467.
 38. Kehrer M, Goelz R, Krägeloh-Mann I, Schöning M. Measurement of volume of cerebral blood flow in healthy preterm and term neonates with ultrasound. *Lancet* 2002;360(9347):1749-1750.
 39. Riccabona M, Nelson TR, Weitzer C, Resch B, Pretorius DP. Potential of three-dimensional ultrasound in neonatal and paediatric neurosonography. *Eur Radiol* 2003;13(9):2082-2093.
 40. Knieling F, Waldner MJ, Goertz RS, et al. Early response to anti-tumoral treatment in hepatocellular carcinoma--can quantitative contrast-enhanced ultrasound predict outcome? *Ultraschall Med* 2013;34(1):38-46.